Available online at www.sciencedirect.com

ScienceDirect

Energy Procedia 142 (2017) 3407–3414

Energy Procedia

www.elsevier.com/locate/procedia

9th International Conference on Applied Energy, ICAE2017, 21-24 August 2017, Cardiff, UK

Mass transfer characteristics of the liquid film flow in a rotating packed bed for CO_2 capture: A micro-scale CFD analysis

Peng Xie, Xuesong Lu, Derek Ingham, Lin Ma*, Mohamed Pourkashanian

Energy2050, Mechanical Engineering, Faculty of Engineering, University of Sheffield, Sheffield S10 2TN, UK

Abstract

Rotating packed beds (RPBs) are promising to be employed for CO_2 capture from the flue gas due to their high mass transfer efficiency. Therefore, good predictions of the mass transfer characteristics for RPBs are crucial for their design. In this paper, a method based on CFD simulation is proposed to investigate the liquid film flows and mass transfer characteristics within RPBs. Local mass transfer coefficients along the radial direction of an RPB have been obtained. The results obtained show that high surface roughness and high rotational speed enhance the CO_2 absorption into the liquid film, thus generating a high mass transfer coefficient, and the larger the RPB radial position, the higher the mass transfer coefficient.

Peer-review under responsibility of the scientific committee of the 9th International Conference on Applied Energy.

Keywords: Rotating packed bed; CFD; CO_2 capture; liquid film flow; mass transfer; VOF model

1. Introduction

The rotating packed bed (RPB), as a novel process intensification (PI) technology, was first proposed by Ramshaw and Mallinson in 1981 [1]. As shown in Fig. 1(a), the RPB uses a rotating part to create a high centrifugal field. The liquid is injected into the central region of the RPB and it is split into thin films, tiny droplets, etc., and therefore, a large rapid updating contact area exists between the gas and liquid phases, which enhances the mass transfer processes. Due to these merits, the RPB has been widely employed in absorption, desorption, distillation, etc. Recently, the advantages of employing RPBs in the post-combustion CO_2 capture (PCC) process among different PI technologies have been demonstrated [2].

* Corresponding author. Tel.: +44 114 215 7212.
E-mail address: lin.ma@sheffield.ac.uk

1876-6102
Peer-review under responsibility of the scientific committee of the 9th International Conference on Applied Energy.
10.1016/j.egypro.2017.12.478

Some fundamental investigations on the mass transfer phenomena in RPBs have also been performed experimentally since the 1980s [3, 4], however, long experimental periods and expensive cost limit experimental methods from being extensively employed for the large-scale RPB design. In addition, the high rotational speed of the rotor and limited space inside the packing regions make it almost impossible to insert any measuring instruments without interrupting the liquid flow and therefore it is very difficult to reveal local information of the RPB, which dramatically restricts a deep understanding of the RPB. It is thus necessary to develop an efficient and economical technique for the analysis of the mass transfer phenomena in large-scale RPBs. Fortunately, CFD simulations can cover the disadvantages of experimental researches to a great extent. For example, Shi et al. [5] investigated the gas-liquid two-phase flow in RPBs through using the Volume of Fluid (VOF) multiphase flow model. Further, Yang et al. [6] developed a CFD model based on the VOF model to analyze the mass transfer of a vacuum deaeration process in a small RPB. Xie et al. [7] analysed the liquid flow behaviour in an RPB with wire mesh packings for CO_2 capture through CFD modelling. Although many simplifications have been made in these models, restricted by the computational cost, it is still very difficult to employ such an overall CFD model to investigate a large-scale RPB. This is mainly due to the multiscale geometric characteristics of the RPB and the tinny feature size of the liquid in the RPB. Therefore, it is very difficult to produce a macro-scale CFD model that captures every detail of the flow in the RPB. Similar to the multiscale modelling of a packed column [8, 9], the modelling of an RPB also can be divided into several different scales depending on the research emphasis. CFD simulation has the advantages in investigating the micro-scale transient flow and mass transfer characteristics in the RPB because the transient gas-liquid interface can be clearly tracked using the VOF method and mass transfer also can be implemented in the VOF model.

Thus, the objective of the paper is to investigate the effect of rotational speed and the surface texture on the mass transfer in the RPB through micro-scale CFD modelling. In this paper, the commercial software ANSYS FLUENT 17.2 was used to simulate the micro-scale CO_2 physical mass transfer process in the liquid film in the RPB. The VOF model is implemented to calculate the flow field and capture the gas-liquid interface in the RPB. The concentration of the CO_2 in the liquid films was solved by employing convection-diffusion equations.

2. Numerical simulation

2.1. Geometry model and governing equations

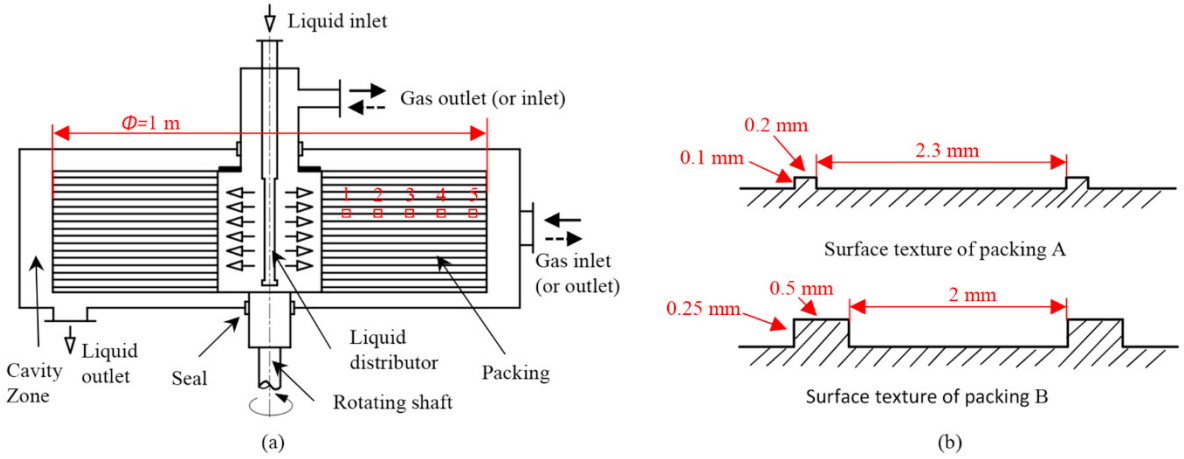

Fig. 1. (a) Schematic diagram of an RPB; (b) Schematic diagram of two packing surface textures.

As shown in Fig. 1(a), an RPB with outer diameter of 1 m is investigated in this paper, and the metal packing sheet is cut into an annular shape and stacked in the packing region to form a firm packed bed. As marked by the red squares in Fig. 1(a), packings that are located at five equally spaced positions along the radial direction are selected to build up micro-scale models. The radial positions of the five calculation points are from 0.1 m to 0.5 m, and at each point,

packings within a length of 20 mm are simulated. Two surface textures with different feature sizes are simulated in this paper, as shown in Fig. 1(b). In order to explore the liquid flow and mass transfer within the liquid films in the RPB, the following basic assumptions are adopted:

(i) The surface textures of the packing are identical along the radial direction.

(ii) The gravity and Coriolis force in the RPB are much weaker than the centrifugal force and therefore they are ignored.

(iii) Liquid films are captured by the packing surface and it flows along the radial direction under the action of the centrifugal force.

(iv) In each case, the centrifugal force is assumed constant because of the short radial variation compared to the radius of the RPB.

Based on these assumptions, the flow in each position can be regarded as a 2D free surface liquid film flow and the calculation domain is shown in Fig. 2.

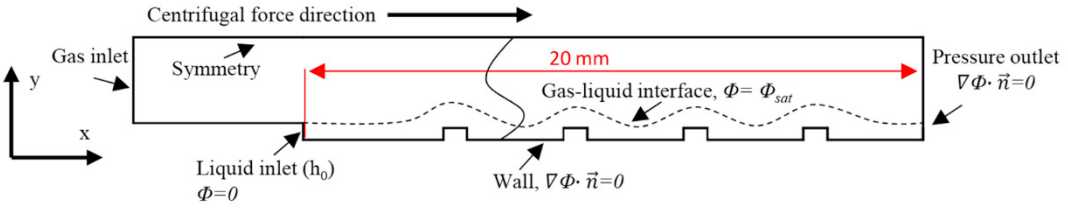

Fig. 2. Schematic diagram of the 2D calculation domain and boundary conditions.

The thin liquid film flow in this work is considered to be laminar, incompressible, Newtonian and isothermal flow. The VOF model is used to study the flow and the flow governing equations are as follows:

The continuous equation

$$\frac{\partial\rho}{\partial t}+\nabla\cdot\left(\rho\vec{v}\right)=0 \tag{1}$$

The momentum conservation equation

$$\frac{\partial}{\partial t}\left(\rho\vec{v}\right)+\nabla\cdot\left(\rho\vec{v}\vec{v}\right)=-\nabla p+\nabla\cdot\left[\mu\left(\nabla\vec{v}+\nabla\vec{v}^{T}\right)\right]+\rho\vec{g}'+F_{vol} \tag{2}$$

where the $g'=r\omega^2$, ω is the rotational speed of the RPB, r is the radial position and F_{vol} is the source term that takes into account the surface tension through the CSF (Continuum Surface Force) model [10].

The volume fraction equation

$$\frac{\partial}{\partial t}\left(\alpha_L\rho_L\right)+\nabla\cdot\left(\alpha_L\rho_L\vec{v}_L\right)=0 \tag{3}$$

In addition, the volume fraction of the primary phase is computed based on $\alpha_G=1-\alpha_L$. The fluid properties are volume-averaged values:

$$\rho=\alpha_L\rho_L+\left(1-\alpha_L\right)\rho_g \tag{4}$$

$$\mu=\alpha_L\mu_L+\left(1-\alpha_L\right)\mu_g \tag{5}$$

The transport equation for the CO_2 mass transport in the liquid film is given by

$$\frac{\partial}{\partial t}\left(\alpha_L \rho_L \phi\right) + \nabla \cdot \left(\alpha_L \rho_L \vec{v}_L \phi - \alpha_L \rho_L D \nabla \phi\right) = 0 \tag{6}$$

where $\phi = c$, and it is the concentration of gas tracers dissolved in the liquid phase, and D is the gas diffusion coefficient in the liquid phase.

2.2. Boundary conditions

The locations and some of the conditions on the boundaries are shown in Fig. 2. Because of the increasing flow space along the radial direction in the RPB, the liquid load varies at different radial positions. In addition, the centrifugal force is different at different radii, thus the liquid film thickness and the liquid velocity changes at different radial positions. Therefore, different boundary conditions are adopted at different radial positions. As for the liquid inlet, the thickness of the liquid film is specified by the Nusselt theory [11], and it is expressed as follows:

$$h_0 = \left(\frac{3\mu_L q_L}{\rho_L g'}\right)^{1/3} \tag{7}$$

where the q_L is the specific flow rate, and it is calculated using

$$q_L = \frac{Q_L}{2\pi r h a_p} \tag{8}$$

where Q_L is the total liquid load of the RPB, and a_p is the surface area of the packing per unit volume of the bed. Then the average liquid inlet velocity is calculated by $u_0 = q_L/h_0$.

The CO_2 phase enters into the computational domain from the rest of the inlet and its velocity can be assumed to be the same as the liquid velocity. As for the outlet conditions, the pressure outlet with a zero gauge pressure is set. At the surface of the wall, a no-slip condition is applied.

For description of CO_2 absorption into the liquid from the gas phase, due to the mass transfer resistance in the gas phase being small, the liquid at the gas-liquid interface is assumed to be always in its saturation state, and the CO_2 saturation concentration at the interface (c_{sat}) is calculated from Henry's law [12]. For the liquid inlet, the CO_2 concentration is assumed zero and for the outlet and the wall, zero flux conditions are specified.

The simulation is performed under a typical RPB operation condition as $Q_L = 1.35 \times 10^{-3}\ m^3/s$, and rotational speed N ranging from 100 rpm to 400 rpm. The specific area of the packing a_p is 754 m^2/m^3. The physical properties of the liquid and gas used in this paper are specified as ρ_L =1015.5 kg/m^3, μ_L = 0.00696 Pa.s, σ_L =0.0489 N/m, ρ_G =1.977 kg/m^3, $D = 1.828\times10^{-10}$ m^2/s [13] and c_{sat}=0.129 kg/m^3. These properties can simulate the physical absorption process of 10% CO_2 into a 70 wt% aqueous monoethanolamine (MEA) solution.

2.3. Numerical methods

In the calculation, the PISO scheme is used for pressure–velocity coupling, the PRESTO! scheme is adopted for the pressure discretization and the Geo-Reconstruct method is applied for the spatial discretization of the volume fraction equation. In addition, the scalar transport equation (6) is implemented by the user-defined scalar subroutine (UDS), and the second-order upwind scheme is employed for the solution of the momentum and the CO_2 mass transport equations in the liquid. The user-defined function (UDF) is applied to capture the gas-liquid interface and set up the interfacial concentration.

The local averaged bulk concentration (C_b), the local mass transfer coefficient (K_L), and the mean mass transfer coefficient taken over a length are expressed successively as follows [14]:

$$C_b = \frac{\int_0^{h_0} c dy}{h_0}, \quad K_L = \frac{-D\frac{\partial c}{\partial y}\Big|_{y=i/f}}{C_{i/f} - C_b}, \quad K_{L-mean} = \frac{\int_0^L K_L dx}{L} \tag{9}$$

where c is the local concentration of CO_2, $y=i/f$ indicates the interface position, and L is the length of the calculation domain.

3. Results and discussion

3.1. Model validation

For accurately capturing the gas-liquid interface and simulating the mass transfer behaviour in a thin liquid film, fine computational meshes are required. After a mesh independence study, the size of the mesh no bigger than 0.02 mm in the Y direction and no bigger than 0.08 mm in the X direction can achieve mesh independence. At this arrangement, models have been validated through comparing the liquid flow on a flat plate with Kapitza's experimental shadowgraph [15] and the liquid flow on a micro-baffled plate with Ishikawa et al.'s simulation [16], and good agreements for liquid flow have been achieved. As shown in Fig. 3(a1) and Fig. 3(a2), the similar wave shape of a falling liquid film on a flat surface has been achieved. In addition, Fig. 3(b1) and Fig. 3(b2) show the similar wave surface of a falling film flow on the micro-baffled plate. However, due to the thickness of the liquid film changes significantly at different conditions, also the sizes of the computational meshes would be scaling down based on the liquid film thickness.

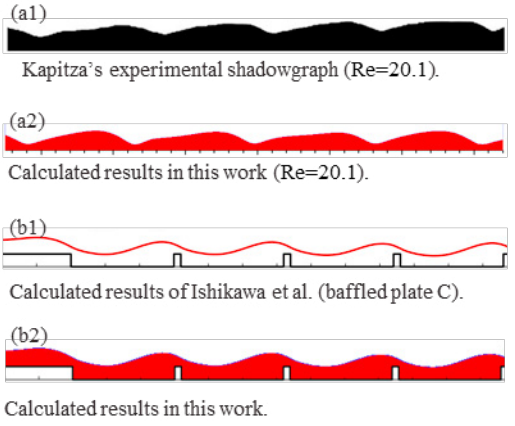

Fig. 3. Simulation results for liquid flow validation.

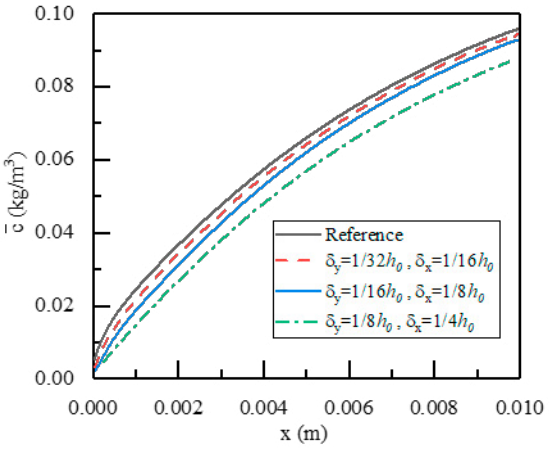

Fig. 4. Simulation results for mass transfer validation.

Since sufficiently resolved experimental measurements for the gas species concentration in thin liquid films are not available, the mass transfer simulation in the VOF model is validated by comparing the simulated species concentration in the liquid films with the results from a reliable theoretical case. The theoretical case is a falling film flow with the film thickness of 1 mm and the length of 10 mm. Under ideal conditions, the flow in this case is laminar flow with a flat liquid surface. Therefore, the shape of the liquid film is fixed on a rectangular single-phase calculation domain and the velocity profile is specified according to the Nusselt's theory [11]. In addition, the physical properties of the liquid used in this case is the same as the 70 wt% MEA solution, the concentration of the dissolved species at the liquid surface is specified as 0.129 kg/m^3 and the gas diffusion coefficient in the liquid phase is specified as

1.828×10^{-5} m^2/s. Then the advection–diffusion equation can be numerically solved for obtaining the species concentration profile inside the liquid film with a high numerical accuracy.

Then several cases of free surface falling film flow with the surface captured by adopting the VOF model are conducted to verify the mass transfer calculation in the VOF model. The inlet velocity profile of the liquid in the VOF model is the same as that specified in the reference case, and the inlet velocity of the gas phase is specified to be equal to the velocity at the liquid surface, which can reduce the influence of the gas phase on the liquid phase. In addition, all the other properties of the liquid in the VOF model are the same as that specified in the reference case to make the liquid film maintain the constant shape as in the reference case.

Through adopting different sizes of meshes in the VOF model, the average CO_2 concentration in the liquid film along the flow direction has been analysed. As can be seen in Fig. 4, when the mesh size is no bigger than 1/16 h_0 in the Y direction and no bigger than 1/8 h_0 in the X direction, the CO_2 concentration profile is almost mesh independent. Therefore, comprehensively considering the calculation precision and calculation time, the mesh size of 1/16 h_0 in the Y direction and 1/8 h_0 in the X direction is regarded as a reasonable fine mesh to predict the CO_2 transportation in the liquid film. Through the above liquid flow and mass transfer validation, we take the view that the CFD modelling method can effectively predict the physical mass transfer process in the thin liquid film.

3.2. Variations of the mass transfer coefficient K_L in the RPB

First of all, the free surface flow at the middle of the bed (R=0.3 m) is investigated under different rotational speeds as well as under a gravitational field in order to investigate the effect of the centrifugal force on the liquid flow and mass transfer characteristics. Fig. 5 shows the instantaneous liquid film flow and CO_2 concentration profiles in the film. As can be seen from Fig. 5, with the increasing of the centrifugal force, the thickness of the liquid film decreases, which means that the liquid holdup on the packing surface decreases. Also the fluctuations of the liquid surface is more severe, which generates a larger surface area. Therefore, the specific surface area of the liquid on the packing surface increases. In addition, under a higher centrifugal field, the inertia force of the liquid in the radial direction increases, and when the liquid impacts on the barriers, severe disordered liquid flow fields appear. As a result, the convection flow inside the liquid film increases, therefore the CO_2 absorption is much faster under a higher centrifugal force.

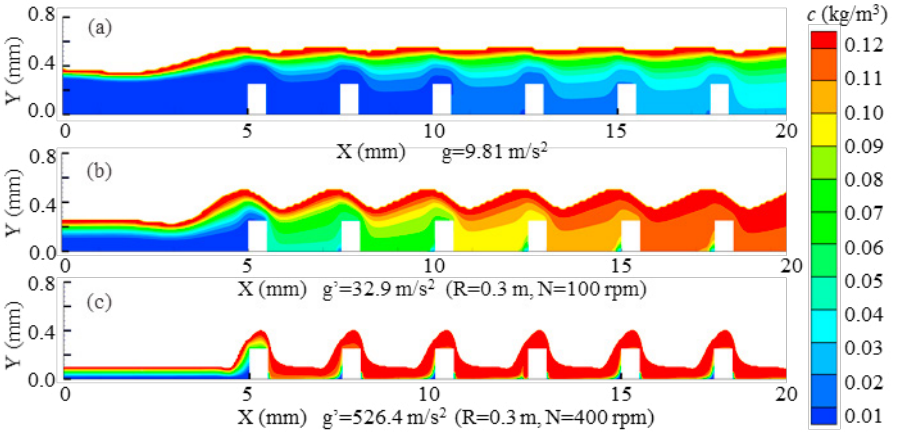

Fig. 5. Instantaneous flow and CO_2 concentration profiles at different gravitational environments.

Further, the whole bed is investigated through using the micro-scale simulation method, which takes into account the varying liquid load and centrifugal force at different radial positions. In Fig. 6, the distribution of the physical mass transfer coefficient (K_L) in the RPB under two rotational speeds (300 and 400 rpm) and using two different packings A and B, are illustrated. It shows that for the same surface texture, K_L increases along the radial direction,

and a higher rotational speed generates a larger K_L, which is extremely clear at a larger radial position. This is mainly because at a large radial position, the centrifugal force is high; meanwhile, the specific liquid flow rate is low due to the increased flow area, both of which result in a thinner liquid film and a higher convective velocity in the liquid film, which can intensify the mass transfer.

In addition, the K_L of the CO_2 absorption on the packing B, which has a higher surface roughness, is larger than the CO_2 absorption on the packing A at the same location and the same rotational speed. This is mainly because when the liquid flows on the packing surface with a high surface roughness, the embossments take a higher percentage of the flow cross-sectional area, and the liquid has to flow over them, and this makes them easier to disturb the flow field and increase the convective velocity in the liquid film, especially in a higher centrifugal field. As a result, the mass transfer rate increases.

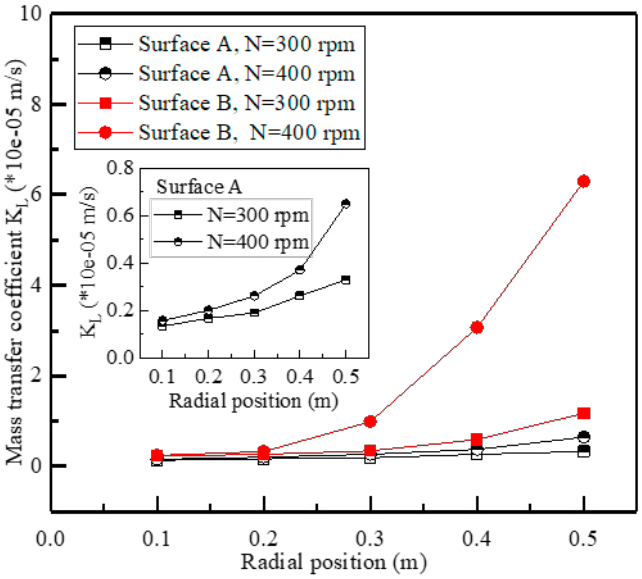

Fig. 6. Variation of K_L along the radial direction in an RPB.

4. Conclusions

This paper has analysed the mass transfer characteristics of liquid film flows in an RPB through the use of micro-scale CFD modelling. The liquid film flow and mass transfer modelling methods have been verified by comparing simulation results with experimental measurements and theoretical investigations. Local liquid film mass transfer coefficients in the RPB have been obtained. The results show that under the simulation conditions, a higher rotational speed enhances the CO_2 absorption into the liquid films due to the increased centrifugal force, which increases the convective velocity in the liquid film and increases the specific surface area of the liquid on the packing surface. The liquid film mass transfer coefficients increase along the radial direction in the RPB because of the higher centrifugal force and the lower specific liquid load. In addition, high surface roughness can increase the mass transfer coefficient, especially in a high centrifugal field. Under the simulation conditions, high centrifugal force and high surface roughness have combined effects on the mass transfer intensification. The simulation results in a deeper understanding on the liquid film flow and mass transfer characteristics in an RPB. This method can assist in the analysis and design of large scale and high efficient RPBs for CO_2 capture.

Acknowledgements

P. Xie would like to acknowledge the China Scholarship Council and the University of Sheffield for funding his research studies. The authors also acknowledge the support from the EPSRC grant (EP/M001458/2).

References

[1] C. Ramshaw, R.H. Mallinson, Mass transfer process, US Patent No. 4283255, 1981.

[2] M. Wang, A.S. Joel, C. Ramshaw, D. Eimer, N.M. Musa, Process intensification for post-combustion CO_2 capture with chemical absorption: A critical review, Appl. Energy, 158 (2015) 275-291.

[3] M.S. Jassim, G. Rochelle, D. Eimer, C. Ramshaw, Carbon dioxide absorption and desorption in aqueous monoethanolamine solutions in a rotating packed bed, Ind. Eng. Chem. Res., 46 (2007) 2823-2833.

[4] B.C. Sun, H.K. Zou, G.W. Chu, L. Shao, Z.Q. Zeng, J.F. Chen, Determination of mass-transfer coefficient of CO_2 in NH_3 and CO_2 absorption by materials balance in a rotating packed bed, Ind. Eng. Chem. Res., 51 (2012) 10949-10954.

[5] X. Shi, Y. Xiang, L.X. Wen, J.F. Chen, CFD analysis of liquid phase flow in a rotating packed bed reactor, Chem. Eng. J., 228 (2013) 1040-1049.

[6] Y.C. Yang, Y. Xiang, G.W. Chu, H.K. Zou, B.C. Sun, M. Arowo, J.F. Chen, CFD modeling of gas-liquid mass transfer process in a rotating packed bed, Chem. Eng. J., 294 (2016) 111-121.

[7] P. Xie, X. Lu, X. Yang, D. Ingham, L. Ma, M. Pourkashanian, Characteristics of liquid flow in a rotating packed bed for CO_2 capture: A CFD analysis, Chem. Eng. Sci., 172 (2017) 216-229.

[8] B. Sun, L. He, B.T. Liu, F. Gu, C.J. Liu, A new multi-scale model based on CFD and macroscopic calculation for corrugated structured packing column, AlChE J., 59 (2013) 3119-3130.

[9] L. Raynal, A. Royon-Lebeaud, A multi-scale approach for CFD calculations of gas-liquid flow within large size column equipped with structured packing, Chem. Eng. Sci., 62 (2007) 7196-7204.

[10] J.U. Brackbill, D.B. Kothe, C. Zemach, A Continuum Method for Modeling Surface-Tension, J. Comput. Phys., 100 (1992) 335-354.

[11] W. Nusselt, Die Oberflachenkondesation des Wasserdamffes the surface condensation of water, Zetrschr. Ver. Deutch. Ing., 60 (1916) 541-546.

[12] A. Penttila, C. Dell'Era, P. Uusi-Kyyny, V. Alopaeus, The Henry's law constant of N2O and CO2 in aqueous binary and ternary amine solutions (MEA, DEA, DIPA, MDEA, and AMP), Fluid Phase Equilibr, 311 (2011) 59-66.

[13] G.F. Versteeg, W.P.M. Vanswaaij, Solubility and Diffusivity of Acid Gases (Co2, N2o) in Aqueous Alkanolamine Solutions, J. Chem. Eng. Data, 33 (1988) 29-34.

[14] Z.F. Xu, B.C. Khoo, N.E. Wijeysundera, Mass transfer across the falling film: Simulations and experiments, Chem. Eng. Sci., 63 (2008) 2559-2575.

[15] P.L. Kapitza, Wave flow of thin layers of viscous liquid. Part I. Free flow, Zhurnal Eksperimentalnoi i Teoreticheskoi Fiziki, 18 (1948) 3-18.

[16] H. Ishikawa, S. Ookawara, S. Yoshikawa, A study of wavy falling film flow on micro-baffled plate, Chem. Eng. Sci., 149 (2016) 104-116.